PROTEINS: Structure, Function, and Genetics 24:485–494 (1996)

# Time-Resolved Fluorescence Study of a Calcium-Induced Conformational Change in Prothrombin Fragment 1

**Martin Hof,[1] Graham R. Fleming,[2] and Vlastimil Fidler[1,3]**

*[1]Department of Physical Chemistry, Charles University, 12840 Prague 2, Czech Republic; [2]Department of Chemistry, University of Chicago, Chicago, Illinois 60637; [3]Department of Physical Electronics, Czech Technical University in Prague, 18000 Praha 8, Czech Republic*

***ABSTRACT*** **The wavelength dependent fluorescence decay properties of bovine prothrombin fragment 1 have been investigated employing a picosecond time-correlated single photon counting technique. All observations are discussed with using the crystal structure (Soriano-Garcia et al., Biochemistry 31:2554–2566, 1992). Fluorescence lifetimes distribution and conventional multiexponential analysis, as well as acrylamide quenching studies lead to the identification of six distinguishable tryptophan excited-states. Accessibility to the quencher and the known structure are used to associate a fluorescence decay of the tryptophan present in the Gla domain (Trp42) with two red shifted components (2.3 and 4.9 ns). The two kringle domain tryptophans (Trp90 and Trp126) exhibit four decay times (0.06, 0.24, 0.68, and 2.3 ns), which are blue shifted. The calcium-induced fluorescence quenching is a result of static quenching: the five decay times remain unchanged, whereas the fluorescence intensity of Trp42 is decreased. The static quenching process is a consequence of a ground state interaction between the Cys18-Cys23 disulfide bridge and Trp42. The monomolecular equilibrium constant for this disulfide-π-electron interaction is found as 4.8.** © 1996 Wiley-Liss, Inc.

**Key words: static quenching, tryptophan-disulfide interaction, lifetimes distribution analysis, blood coagulation, factor II, γ-carboxyglutamic acid domain**

## INTRODUCTION

Bovine prothrombin (factor II), the zymogen of thrombin (factor IIa), is a single polypeptide chain plasma glycoprotein. It serves as the substrate of the prothrombinase complex, which consists of factor Xa, factor Va, calcium ions, and anionic phospholipid surfaces.[1] The 1–156 N-terminal of prothrombin is named fragment 1 and is believed to be the region predominately responsible for the metal ion and membrane binding properties of prothrombin. Several coagulation factors (VII, IX, X, and the proteins C, S, and Z) display extensive homology to the residues 1 to 48 of prothrombin among their N-termini;[2] each of these domains contains nine to 12 γ-carboxyglutamic acid residues (Gla).

The structure of BF1 may be divided into a "Gla domain," which contains 10 Gla residues, and a domain with three disulfide linkages known as the "kringle" region. BF1 contains three tryptophan residues (Trp42, Trp90, and Trp126). The Gla domain reveals a single tryptophan at position Trp42. A surface accessibility of $133 \times 10^{-20}$ m$^2$ indicates partial solvent exposure of Trp42 in apo-BF1.[3] The core of the tertiary structure of the highly ordered kringle is the central cluster formed by Trp90, Trp126, Tyr128, Pro98, and Pro118.[4] The kringle tryptophans are located 0.9 nm apart from each other, whereas the distance of Trp90 and Trp126 to Trp42 is about 2.5 nm and 2.3 nm, respectively. Due to the calculated solvent accessibilities of $4 \times 10^{-20}$ m$^2$ for Trp90 and Trp126 in apo-BF1, the kringle tryptophans appear to be solvent inaccessible.[4]

Seven calcium ions bind to the Gla domain of prothrombin and its fragment 1 in a partially positive cooperative manner, and form the native conformation required for membrane binding. The calcium ions are chelated by nine Gla residues (for illustration, see Soriano-Garcia et al.,[5] Fig. 2). Ca-1 to Ca-5 are electronically neutral, whereas Ca-6 and Ca-7, which form a cluster with Gla residues 15, 20, 21 involving the Cys18–Cys23 hexapeptide disulfide loop, possess a positive charge, and are therefore candidates for the binding to negatively charged phospholipid head groups. In addition, Gla15 and Gla21 are reasonably situated to enter in further

Abbreviations: apo-BF1, the absence of calcium ions; BF1, bovine prothrombin residues 1-156; Ca-BF1, the presence of calcium ions; DAS, decay-associated spectra; Gla, γ-carboxyglutamic acid; Tris, tris(hydroxymethyl)aminomethane.

Received May 19, 1995; revision accepted August 24, 1995.

Address reprint requests to Dr. Martin Hof, Department of Physical Chemistry, Charles University, Albertov 2030, 12840 Prague 2, Czech Republic.

calcium ion-phospholipid interactions.[5] Although experimental data indicate a weak calcium binding site in the kringle domain,[6,7] structural evidence for such a site was not reported.[5]

The calcium-induced conformational change of BF1 can be observed experimentally by circular dichroism[8] and by the intrinsic fluorescence quenching paralleling the conformational change in two steps.[9–11] The fluorescence quenching (in total 40%) is believed to be due to the stabilization of interaction between Cys18-Cys23 and the aromatic cluster Phe41, Trp42, and Tyr45 by a trans to cis isomerization of Pro54.[3,5] It was concluded that along with the establishing of this disulfide-π-electron interaction, a more hydrophobic environment of Trp42 is created. The increase in the hydrophobicity was believed to be the reason for the decrease in the tryptophan quantum yield. A contribution of the kringle domain to the fluorescence quenching could be excluded by the invariance of the solvent accessible surface areas of Trp90 and Trp126 upon calcium addition.

Studies involving factors IX and X, which contain epidermal growth factor-like domains rather than kringle domains, reveal an increase in the fluorescence intensity at low calcium concentrations and a BF1-comparable decrease at higher calcium concentrations.[12–14] The overall fluorescence decrease upon calcium addition was assigned to an increase in the hydrophobicity of the environment of the Gla tryptophan by investigating the steady-state spectra of the isolated fragments of these proteins.

In this study, we investigate the calcium-induced conformational change of BF1 by picosecond time-resolved spectroscopy of the three BF1 tryptophans. Using this technique, changes in the microenvironment of the individual tryptophans can be separated from each other without cleaving BF1 into the isolated Gla and kringle domains or using site-directed mutagenesis. A detailed analysis of the wavelength dependent fluorescence decays, using different models of lifetimes distributions, global analysis, and acrylamide quenching studies, leads to an assignment of the observed fluorescence decay time domains. Addition of $CaCl_2$ leads to a faster decay of the tryptophan fluorescence, but does not change the fluorescence decay times, as expected from the hypothesis that a decrease in the hydrophilicity of the Trp42 environment causes the quantum yield decrease.[3,5] A static quenching mechanism of the Trp42 fluorescence, based on an equilibrium interaction between Trp42 and the Cys18–Cys23 disulfide linkage, is shown to be responsible for the fluorescence decrease.

For a general introduction to tryptophan fluorescence, the reader is referred to two review articles.[15,16] The principles of the single photon counting technique are summarized in two books.[17,18]

## MATERIALS AND METHODS

### Prothrombin Fragment 1

Bovine prothrombin fragment 1 was purified as previously described.[19–21] Sodium dodecyl sulfate-polyacrylamide gel electrophoresis indicated >95% purity. Concentrations were determined by ultraviolet spectrophotometry at 280 nm ($\varepsilon$ = 1.05 ml $mg^{-1}$ $cm^{-1}$, molecular mass = 23 kDa). Protein solutions were stored in Tris-buffered saline (0.05 M Tris, 0.1 M NaCl, pH = 7.4) at −70°C until immediately before use. Experiments were carried out at a concentration of 4 μM BF1 in Tris-buffered saline (0.01 M Tris, 0.1 M NaCl, pH = 7.4) at 25°C. The $CaCl_2$ concentrations in the Ca-BF1 samples were 4.5 mM. The fluorescence was measured 30 minutes after $CaCl_2$ addition.

### Acrylamide

The acrylamide (Sigma Chemical Co., St. Louis, MO) quenching experiments were performed by adding successively small volumes (5–40 μl) of 5.6 M acrylamide solution (pH = 7.4) to the protein solutions.

### Fluorescence Measurements

Corrected fluorescence spectra were obtained on a SLM 8,000 spectrofluorometer (Urbana, IL) using a "magic angle" configuration. Bandwidths of 2 nm were set for the excitation as well as for the emission.

The fluorescence lifetime measurements were performed with a single photon counting technique as described elsewhere.[22,23] The excitation at 295 nm was vertically polarized. The emission was detected after passing through a "magic angle" polarizer and a J-Y H10 (Instrument SA Inc., Metochen, NJ) monochromator with a 2 nm band pass, on a Hamamatsu R1645U (Bridgewater, NJ) microchannel plate photomultiplier. Fluorescence decays were collected with 10,000 to 40,000 counts in the peak. The time scales were 14.3, 25.5, and 62.4 ps per channel, 512 channels collected. The instrument response functions (55 ps full width at half maximum) were measured using a light scattering solution of a non-diary coffee creamer. The fluorescence decays of apo- and Ca-BF1 were collected from 300 to 425 nm in 5 nm steps. The acrylamide quenching was investigated at 300, 310, 330, 350, 370, 390, and 400 nm. Blank experiments using Tris-buffered saline were performed to exclude distortions by scattered light. The intensity of the scattered light at 300 nm, as well as at the $H_2O$-Raman band, was negligible.

### Data Analysis

For the basic multiexponential analysis, a nonlinear least-squares iterative reconvolution procedure was used. The program is based on the Marquardt Levenberg algorithm[24] and the optimization

includes stray light and time shift.[25] To account for the possibility of a continuous distribution of lifetimes, the data were fit using the symmetric Lorentzian distribution and the asymmetric Kohlrausch-Williams-Watts distribution.[25]

A modified version of the commercially available Edinburgh Analytical Instruments (Edinburgh, UK) global analysis program was employed to simultaneously reconvolve the decays collected at different emission wavelengths. The program uses the Marquardt Levenberg algorithm. The wavelength dependent sets of fluorescence decays were analyzed by linking the lifetime values.

To characterize the number of classes of fluorescence lifetimes, the Edinburgh Analytical Instruments distribution program was used. The program is based on the minimum energy method where the lifetimes are equally spaced on a logarithmic scale.

All three programs use reduced $\chi^2$ as a criterion for the goodness of fit evaluation. Furthermore, the quality of the fit was judged by weighted residuals and the Durbin-Watson parameter. In the case of the global analysis, the mean reduced $\chi^2$-value ($\chi^{2(\text{Global})}$) was used to evaluate the goodness of the fit.

Decay-associated spectra (DAS) were obtained by combining the time-resolved data with the steady-state emission spectra, as described elsewhere.[15] To determine the emission maxima, the DAS were fit to log-normal distribution functions.[26] Global analysis of the wavelength dependent decays at given acrylamide concentrations have been performed to determine the quenched fluorescence lifetimes. The acrylamide quenching of each excited-state lifetime was analyzed using the Stern-Volmer equation.[27,28]

## RESULTS

### Characterization of the Fluorescence Decay of Apo-Fragment 1

To describe the fluorescence decays of tryptophans in proteins at a single emission wavelength, two possibilities have to be considered. Either the intensity decay is interpreted by a set of separate classes of lifetimes or, as in recent publications,[29–32] by a (broad) continuous lifetimes distribution model. Although the second case seemed to be unlikely for a three tryptophans containing protein, the fluorescence decays of apo-BF1 were fit using the symmetric Lorentzian distribution profile and the asymmetric Kohlrausch-Williams-Watts distribution. Unacceptable high $\chi^2$-values (>2.0) led to the conclusion that excitation light at 295 nm creates more than one class of tryptophan excited-states.

To characterize the number of separate classes of lifetimes, the Edinburgh Analytical Instruments distribution program was applied. In contradiction to the continuous distribution models used above, there is no "a priori" assumption about the distribution shape. The fluorescence decay is fit using a sum

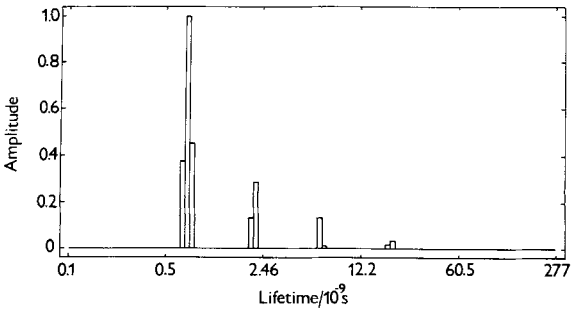


Fig. 1. Amplitude profile of the fluorescence lifetimes distribution of a defined 4-exponential decay, produced by the Edinburgh Analytical Instruments distribution program. In order to create a defined 4-exponential decay, the fluorescence decays of four standard fluorophores with monoexponential decays were superimposed computationally. The standards (1,4-diphenyl-1,3-butadiene, 2,5-diphenyloxazole, anthracene, and pyrene, all in cyclohexane) have been selected to span for tryptophan relevant lifetime range (0.56±0.01 ns, 1.31±0.01 ns, 5.09±0.01 ns, and 19.50±0.01 ns, respectively). The mean lifetime values from the distribution fits are 0.72 ns, 2.1 ns, 6.2 ns, and 20.0 ns.

of 100 lifetime values. The best fit is determined by the minimum energy method. Since no application of a distribution of lifetimes program based on the minimum energy method has been published so far, the significance and accuracy of obtained lifetime profiles was tested: the fluorescence decays of four standards (1,4-diphenyl-1,3-butadiene, 2,5-diphenyloxazole, anthracene, and pyrene, all in cyclohexane) with different lifetime values (0.56±0.01 ns, 1.31±0.01 ns, 5.09±0.01 ns, and 19.50±0.01 ns, respectively) were accumulated to simulate a defined 4-exponential decay. The signal-to-noise ratio was comparable to the BF1 experiments. Figure 1 demonstrates that the existence of four different relevant lifetime classes can be resolved. However, the width of the found four lifetime distributions is substantially larger than the four standard deviations that result from the conventional 4-exponential fit.

When applied to the fluorescence decays of apo-BF1, the analysis of the decays detected at 315–385 nm yielded five lifetime classes. The values of the lifetime centers are identical for all emission wavelengths within the experimental error, while the fractional amplitudes vary. The over all wavelength averaged values are 0.06 ns (component A), 0.25 ns (B), 0.74 ns (C), 2.5 ns (D), and 5.3 ns (E). The analysis at the blue (300 to 310 nm) and red edge (390 to 425 nm) of the emission spectrum resulted in four lifetime classes. This can be explained by the decrease of the fractional intensities of component A and E at the red and blue edge of the spectrum, respectively. The distribution widths of the five apo-BF1 components (Fig. 2) are significantly larger than those of the defined 4-exponential decay (Fig. 1). Since the signal-to-noise ratio in both experiments was comparable, the broadening of the apo-BF1 components might indicate a ground state heterogeneity of the individual tryptophans. However,

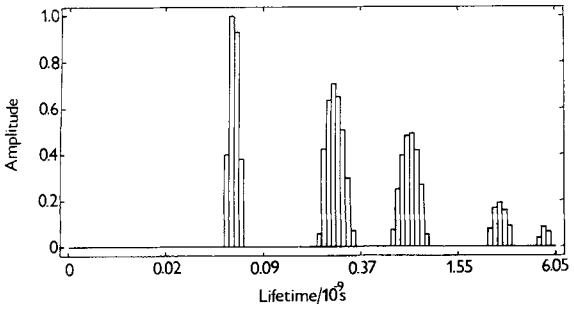


Fig. 2. Amplitude profile of the fluorescence lifetimes distribution of apo-BF1 fluorescence decay ($\lambda_{ex}$ = 295 nm; $\lambda_{em}$ = 330 nm; 4 μM in Tris-buffer) resulting from Edinburgh Analytical Instruments distribution analysis. The resulting mean lifetimes for this measurement are 0.06 ns, 0.26 ns, 0.76 ns, 2.8 ns, and 5.4 ns.

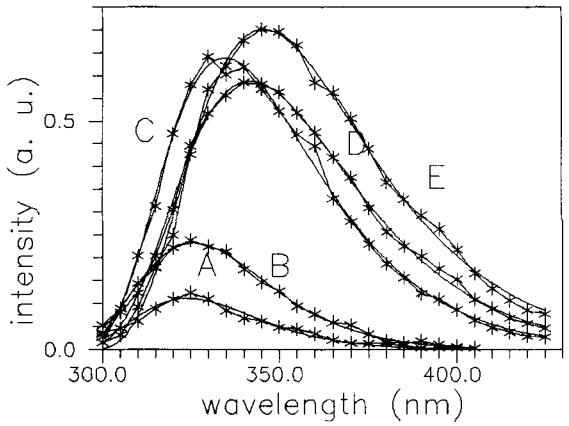


Fig. 3. Decay-associated emission spectra of 4 μM apo-BF1 in Tris-buffer (λex = 295 nm). The fluorescence decay time values are 0.06±0.01 ns (component A), 0.24±0.01 ns (B), 0.68±0.02 ns (C), 2.3±0.2 ns (D), and 4.9±0.3 ns (E). The emission maxima of the log-normal distribution fits are 324.3 nm (A), 325.8 nm (B), 334.8 nm (C), 341.9 nm (D), and 345.5 nm (E). Shown are the experimental points (*) connected by solid lines and the corresponding log-normal distribution fits.

the five components are clearly separated from each other and the resulting widths are small in comparison to those corresponding to proteins for which continuous distributions were discussed.[29–32]

The conventional multiexponential analysis of the wavelength dependent set of the decay curves includes judging the fits by the above mentioned criteria and leads to the same conclusion, i.e., the existence of five components with different emission spectra. Again, the lifetime values were wavelength independent within the experimental error, whereas the amplitudes changed with the wavelength. In conclusion, the existence of five lifetime classes was obtained by the two different iteration methods used, the Marquardt Levenberg algorithm for multiexponential analysis and the minimum energy method for a distribution of lifetimes.

Although the comparison of Figures 1 and 2 indicates that the five lifetime classes in the fluorescence decay of apo-BF1 exhibit significant distribution widths, a global multiexponential analysis of the fluorescence decays has been performed as well. Since the multiexponential analysis yielded constant lifetime values over the emission spectrum, the fluorescence lifetimes were linked. Again, five lifetime components were necessary to reach an acceptable $\chi^{2(\text{Global})}$-value of 1.29. The fluorescence decay time values obtained this way are 0.06±0.01 ns (component A), 0.24±0.01 ns (B), 0.68±0.02 ns (C), 2.3±0.2 ns (D), and 4.9±0.3 ns (E). The standard deviations resulting from the global analysis were significantly smaller in comparison with the unlinked multiexponential analysis of individual decays. The decay-associated spectra of apo-BF1, which were calculated from the steady-state intensities and the fractional intensities obtained by the global analysis, are shown in Figure 3. The emission maxima of the log-normal fits of the five components are 324.3 nm (A), 325.8 nm (B), 334.8 nm (C), 341.9 nm (D), and 345.5 nm (E).

## Acrylamide Quenching of Apo-Fragment 1 Fluorescence

Since structural data shows a huge difference in solvent accessibilities for the kringle tryptophans ($4\times10^{-20}$ m$^2$ for Trp90 and Trp126) and the Gla tryptophan ($133\times10^{-20}$ m$^2$ for Trp42),[3,4] acrylamide quenching studies were performed to assign the five lifetimes to the two types of tryptophans. Acrylamide was added successively up to a concentration of 0.7 M. The fluorescence decays were measured at seven different wavelengths (300, 310, 330, 350, 370, 390, and 400 nm). To determine the quenched lifetime values at each acrylamide concentration, the seven decays detected at different emission wavelength were reconvoluted using a 5-exponential global analysis with linked fluorescence lifetimes. The lifetime value of component A was held constant, since its value of 60 ps is very close to the time resolution of the single photon counting apparatus used and thus a possible acrylamide quenching of A would not be resolved. Linking the decay times of component B, C, D, and E led to unacceptable high $\chi^{2(\text{Global})}$-values (>1.7) for all acrylamide concentrations, indicating that the acrylamide quenching efficiency of at least one component is wavelength dependent. When the lifetime values of D are determined unlinked while B, C, and E are linked, the qualities of the global fits improve significantly ($\chi^{2(\text{Global})}$-values < 1.4). The qualities of the fits appear not to be sensitive to unlinked iteration of component B, C, and E. The changes in the lifetimes were analyzed in terms of the Stern-Volmer equation to yield the bimolecular quenching constant k(q).

The lifetime value of component B is independent

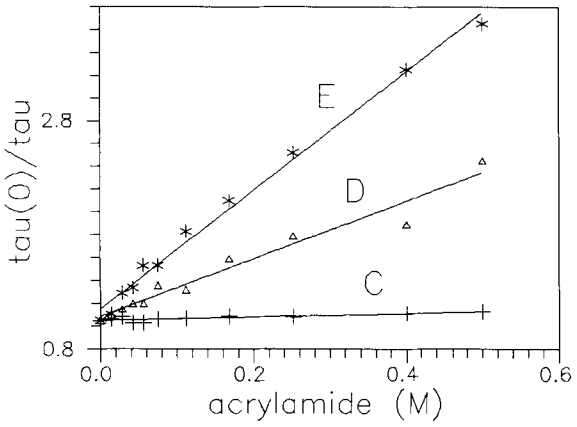


Fig. 4. Stern-Volmer plot for the fluorescence decay of the components C (+), D (△) (at 400 nm), and E (*) of 4 μM apo-BF1 quenched by acrylamide. The resulting bimolecular quenching constants are: $k(q) = 1.1 \pm 0.2 \times 10^9\ M^{-1}\ s^{-1}$ (E, global analysis), $k(q) = 1.1 \pm 0.3 \times 10^9\ M^{-1}\ s^{-1}$ (D, at 400 nm), $k(q) = 0.2 \pm 0.2 \times 10^9\ M^{-1}\ s^{-1}$ (C; global analysis).

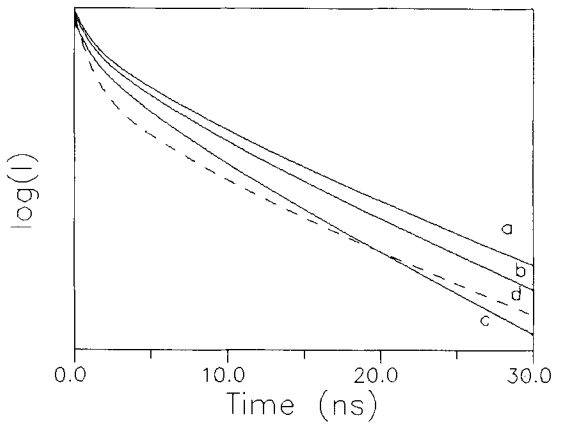


Fig. 5. "Pure" fluorescence decay functions, reconvoluted from the fitted fluorescence decay curves ($\lambda_{em}$ = 400 nm, $\chi^2 < 1.1$); the curve a is the decay of 4 μM apo-BF1, curve b and c are the decays after addition of acrylamide (0.014 M and 0.042 M for b and c, respectively; dynamic quenching); curve d (dashed lines) is the decay of Ca-BF1 (4.5 mM $CaCl_2$; static quenching).

on acrylamide addition up to a concentration of 0.7 M acrylamide. Taking into account an uncertainty in the determination of this lifetime value of about 5%, the bimolecular quenching constant k(q) appears to be smaller than $0.5 \times 10^9\ M^{-1}\ s^{-1}$, indicating that a little or not solvent-accessible tryptophan[15] fluoresce with a lifetime of 0.24 ns. The globally determined lifetimes of component C (0.68 ns) show very weak dependence on acrylamide addition. A quenching constant k(q) of $0.2 \pm 0.2 \times 10^9\ M^{-1}\ s^{-1}$ implies that the corresponding fluorescing tryptophan is buried in the protein.[15] The quenching of component D (2.3 ns) is wavelength dependent. At 400 nm the Stern-Volmer analysis gives a quenching constant k(q) of $1.1 \pm 0.3 \times 10^9\ M^{-1}\ s^{-1}$. At smaller wavelength the Stern-Volmer plot becomes non-linear and the quenching less effective. The component E (4.8 ns) is quenched more than five times faster than C. The k(q)-value of $1.1 \pm 0.2 \times 10^9\ M^{-1}\ s^{-1}$, which is calculated from globally determined lifetimes, implies that a partially exposed tryptophan accounts for component E. The Stern-Volmer plots for component B, D (at 400 nm), and E are shown in Figure 4.

### Global Analysis and Decay-Associated Spectra of Ca-Fragment 1 Fluorescence

The fluorescence decays of Ca-BF1 were detected at different emission wavelengths (300 to 420 nm, 5 nm steps). With $CaCl_2$ present, the fluorescence intensity decays generally much faster than in the case of apo-BF1 (Fig. 5). In order to characterize the decay behavior of Ca-BF1, the same analysis procedure as with apo-BF1 has been performed. Again, five lifetime classes with different emission spectra were found. The $\chi^{2(\text{Global})}$-value for a 5-exponential analysis was 1.24. The obtained fluorescence lifetimes are 0.06±0.01 ns (component A), 0.24±0.01 ns (B), 0.67±0.02 ns (C), 2.3±0.3 ns (D), and 5.1±0.4 ns (E). Therefore, the dramatic shortening of the fluorescence decay of BF1 and the 40% decrease in the quantum yield upon $CaCl_2$ addition cannot be explained by changes in the fluorescence lifetimes. The emission maxima of the DAS log-normal fits are 325.8 nm (component A), 327.2 nm (B), 334.2 nm (C), 337.4 nm (D), and 347.6 nm (E).

Comparison of the DAS of component D and E for apo- and Ca-BF1 (Fig. 6) shows that addition of calcium ions leads to a dramatic decrease of the emission intensities of the 2.3 ns (D) and 5 ns (E) components (maximum intensity (Ca-BF1)/maximum intensity (apo-BF1): 0.17 (E); 0.37 (D)). Whereas the emission maximum of E remains nearly unchanged, $CaCl_2$ addition leads to a significant blue shift of D (341.9 nm to 337.4 nm). Furthermore, the intensity decrease of component E is larger than of D.

Figure 7 compares the DAS of the three subnanosecond components A, B, and C for apo- and Ca-BF1. In all three cases the emission maxima for apo- and Ca-BF1 are identical within the experimental error. The intensity of A and C are unchanged. The increase in the fluorescence intensity of B is small in comparison to the changes in component D and E, but is out of experimental error (maximum intensity (Ca-BF1)/maximum intensity (apo-BF1): 1.51).

## DISCUSSION

The description of the fluorescence decays of apo- and Ca-BF1 by a decay model with five wavelength independent lifetimes results from the distribution of lifetimes analysis (minimum energy method) and the global analysis (Marquardt Levenberg algorithm). Both methods yield essentially identical mean lifetime values. The remarkable agreement of

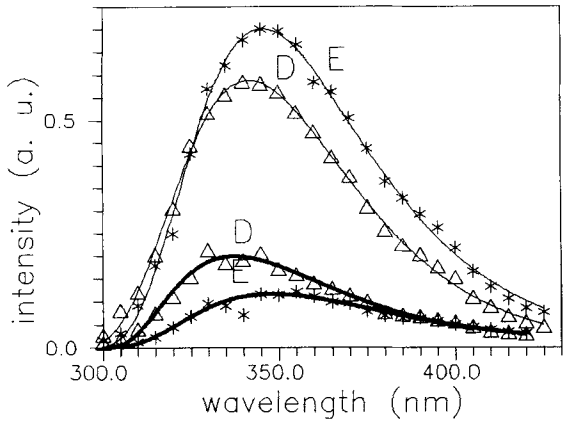


Fig. 6. Decay-associated spectra of components D (△) and E (*) for apo-BF1 (2.3±0.2 ns (D) and 4.9±0.3 ns (E)) and for Ca-BF1 (2.3±0.3 ns (D) and 5.1±0.4 ns (E)). Shown are the experimental points and the log-normal fits to the data. Thick lines represent the decay-associated spectra of Ca-BF1. The emission maxima are 341.9 nm (D) and 345.5 nm (E) for apo-BF1, and 337.4 nm (D) and 347.6 nm (E) for Ca-BF1.

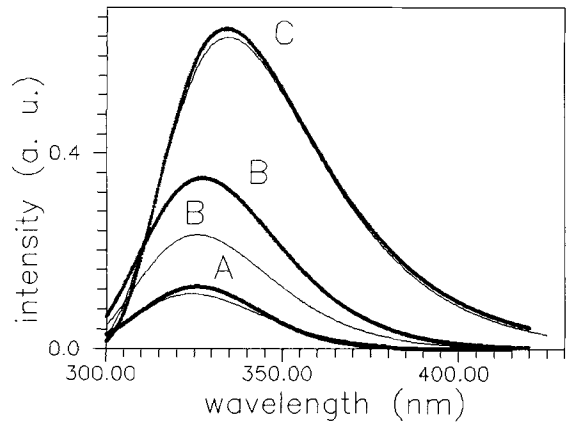


Fig. 7. Decay-associated spectra of components A, B, and C for apo-BF1 (0.06±0.01 ns (A), 0.24±0.01 ns (B), and 0.68±0.02 ns (C)) and for Ca-BF1 (0.06±0.01 ns (A), 0.24±0.01 ns (B), and 0.67±0.02 ns (C)). Shown are the log-normal fits to the data. Thick lines represent the decay-associated spectra of Ca-BF1. The emission maxima are 324.3 nm (A), 325.8 nm (B), and 334.8 nm (C) for apo-BF1, and 325.8 nm (A), 327.2 nm (B), and 334.2 nm (C) for Ca-BF1.

both, very different, analysis methods leads to the conclusion that the fluorescence of the three tryptophans is characterized by at least five different tryptophan excited-states. Contributions of excited-state reactions, as Trp–Trp energy transfer[33–35] or solvent relaxation during the excited-state lifetimes[36–38] are unlikely, since reconvolution fits at the red edge of the emission spectrum do not have any negative fractional amplitudes, and the steady-state emission spectra do not change with red edge excitation (data not shown).[16]

Acrylamide is a quencher widely used for assignment of lifetimes.[28,32,39] The theoretical k(q)-value for a fully exposed polypeptide-tryptophan is about 3 $\times$ $10^9$ $M^{-1}$ $s^{-1}$.[15] Totally buried tryptophans exhibit k(q)-values < 0.2 $\times$ $10^9$ $M^{-1}$ $s^{-1}$.[15] The more than five times larger quenching rate for component E than for C (Fig. 4) reflects the substantial difference in the residue surface accessibilities for the Gla and kringle tryptophans.[3,4] A comparison with k(q)-values of other proteins[28,32,39] supports the conclusion that the 4.9 ns component is due to partially solvent accessible Trp42 (k(q) = 1.1 ± 0.2 $\times$ $10^9$ $M^{-1}$ $s^{-1}$), whereas the 0.68 ns component (k(q) 0.2±0.2 $\times$ $10^9$ $M^{-1}$ $s^{-1}$) was assigned to the kringle tryptophans.

The wavelength dependence of the component D quenching indicates that more than one tryptophan excited-state accounts for D. At 400 nm k(q) is identical to the one determined for compound E (k(q) = 1.1±0.3 $\times$ $10^9$ $M^{-1}$ $s^{-1}$) (Fig. 4) and the quenching efficiency decreases towards the blue edge of the spectrum. It is concluded that both, the kringle and the Gla tryptophan fluoresce with a lifetime of about 2.3 ns. Thus, the wavelength dependent acrylamide quenching of component D leads to the identification of a sixth tryptophan excited-state in BF1.

Due to the limited time resolution, the acrylamide quenching of component B (0.24 ns) is only characterized by an upper limit of the bimolecular quenching rate. Since the quenching of the Gla tryptophan (k(q) = 1.1±0.2 $\times$ $10^9$ $M^{-1}$ $s^{-1}$) is found to be more than twice as effective as the highest possible quenching rate of component B (k(q) < 0.5 $\times$ $10^9$ $M^{-1}$ $s^{-1}$), the 0.24 ns component is assigned to the kringle tryptophans.

A fluorescence decay time is generally determined by the radiative fluorescence lifetime and the rate of nonradiative deactivation processes. Considering the low quantum yields of 0.089 and 0.051 for apo- and Ca-BF1, respectively,[10] the nonradiative rate constants are much higher than the radiative rate constants. Even though, since the radiative lifetime for tryptophan can vary from 10 to 70 ns depending on the environment,[38] a discussion must focus on both, radiative and radiationless deactivation processes. Though there are contradictory results in the literature,[40] a qualitative rule indicates that buried, more blue emitting tryptophans will exhibit shorter radiative lifetimes than those exposed, the more red emitting ones.[27,38,41,42] Therefore, a larger radiative lifetime value for the red emitting Trp42 than for the buried kringle tryptophans might be one reason for the higher fluorescence decay time values of Trp42 (2.3 and 4.9 ns).

Trp42 exhibits two lifetimes (D and E). Assuming that component E (4.9 ns) represents the solvent quenched fluorescence decay of partially exposed Trp42, a collisional quenching by neighboring amino acids may lead to component D (2.3 ns). Since the tertiary structure of BF1 is not resolved for residues 1–35,[4] an assignment of D to a specific Trp42–quencher interaction is not possible. However,

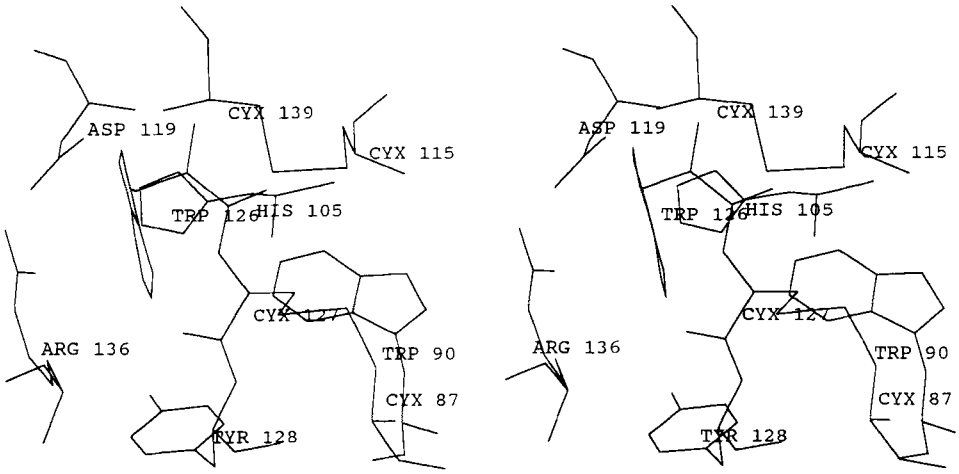


Fig. 8. A depiction of Trp90 and Trp126 and the amino acids, which are in the nearest vicinity of these tryptophans and are known to be a fluorescence quencher. The coordinates were taken from the Brookhaven Protein Data Bank entries[5] and displayed via Hyperchem software (Autodesk Inc., Sausalito, CA).

Tyr45, which is part of an aromatic cluster formed by Phe41, Trp42, and Tyr45,[4] is a candidate for quenching of Trp42 fluorescence.

That Trp90 and Trp126 show shorter lifetimes (components B, C, and D) than Trp42 (D and E) may be due to effective quenching by functional groups in the close vicinity of the kringle tryptophans. The X-ray structure shows a high number of amino acids, that are known to quench tryptophan fluorescence,[38,43,44] nearby Trp90 and Trp126. On the basis of the quenching efficiency classification for amino acids[38,43,44] and on geometrical considerations,[4] we suggest that the following amino acids may be involved in the fluorescence quenching of Trp90 and Trp126: the cysteins of the two inner disulfide bridges (Cys87-Cys127, Cys115-Cys139), Arg136, Asp119, His105, and Tyr128. The spatial orientation of these groups is shown in Figure 8.

The limited time resolution of our experiments prevents an assignment of component A via acrylamide quenching studies. Although a decay time of 60 ps seems to be short for a fluorophore with a radiative lifetime between 10 and 70 ns, the appearance of such a short component is a common feature of many protein studies.[23,28,31,38,45–51]

The calcium-induced conformational change, which is crucial in forming the native conformation demanded by membrane binding, is paralleled by an 40% decrease in the quantum yield,[9–11] by a 9 nm blue shift of the steady-state spectrum (data not shown), and by a shortening of the fluorescence decay (Fig. 5) of BF1. Analysis of the set of Ca-BF1 decays yields the same decay times as in the case of apo-BF1. Therefore, the literature explanations for the observed fluorescence quenching based on shortening of lifetimes due to changes in the hydrophilicity of the Trp42 environment[3,5] leading to more effective dynamic solvent quenching, cannot be accepted. The lifetime invariance together with the decrease in the emission intensity indicate a static quenching mechanism.

The results presented here agree with the conclusion made from the X-ray structure[5] that Trp42 is exclusively responsible for the decrease of the fluorescence intensity. Only the two Trp42 components (D and E) exhibit a strong intensity decrease upon calcium addition (maximum intensity (Ca-BF1)/ maximum intensity (apo-BF1): 0.17 (E); 0.37 (D)). Together with the fact that the decrease in D is smaller than in E, the blue shift of D from 341.9 nm to 337.4 nm (Fig. 6) confirms that D comprises fluorescence of both tryptophan types.

Since the $CaCl_2$ addition stabilizes the interaction between Cys18–Cys23 and the aromatic cluster Phe41, Trp42, and Tyr45,[3,5] we explain the observed static Trp42 quenching by the existence of a ground state equilibrium between a non-fluorescent Trp42–disulfide (Cys18–Cys23) adduct and the free species. The remaining fluorescence of E in Ca-BF1 is due to "free" Trp42. The monomolecular equilibrium constant, which was calculated from the fluorescence maximum intensity values of component E in absence and presence of calcium ions, is 4.8. The static quenching phenomenon is illustrated in Figure 5 by a comparison of the effect of $CaCl_2$ addition with the effect of acrylamide addition (dynamic quenching) on the decay of BF1. Though the Trp42–disulfide interaction was predicted,[5] and a more hydrophobic environment of Trp42 was suggested (calculated solvent accessible areas: 133 and $64 \times 10^{-20}$ $m^2$ for apo- and Ca-BF1, respectively),[3] we did not find any evidence for this hydrophobic environment (lifetimes for component E: $4.9 \pm 0.3$ ns and $5.1 \pm 0.4$ ns for apo- and Ca-BF1, respectively). However, the calculated

changes in the hydrophilicity are, by far, too small to explain the observed 83% intensity decrease of Trp42 fluorescence.

Precedence for a disulfide-tryptophan interaction has been already set by phosphorescence[52,53] and fluorescence[54] studies. Evidence for the static nature of the fluorescence quenching in proteins has been found for tyrosine[55]—as well as for tryptophan[56]—containing polypeptides. Sanyal and coworkers found that the dithiothreitol quenching of 5-methoxyindole, N-acetyl-L-tryptophanamide, melittin, and mastorpan X show a static quenching pattern.[56]

The components A, B, and C do not contribute to the calcium-induced decrease in the quantum yield of BF1 (Fig. 7). A comparison of the spatial organization of the kringle tryptophans and the amino acids, which are known to quench tryptophan fluorescence (Fig. 8), reveals no differences between apo- and Ca-BF1. Since both Trp42 components are quenched upon $CaCl_2$ addition, the invariance of the component A-DAS to $CaCl_2$ addition implies that Trp42 does not fluoresce with a lifetime of 0.06 ns. Therefore, even if A could not be assigned via acrylamide quenching studies, this suggests that A is a fluorescence component of the kringle tryptophans. The components B and C are not quenched by $CaCl_2$ addition, which confirms there are no changes in the environment of the kringle tryptophans. It is to be stressed, that the observed $CaCl_2$ quenching pattern confirms the assignment of the individual components originally based on acrylamide experiments.

Component B exhibits a small increase in the fluorescence intensity (maximum intensity (Ca-BF1)/ maximum intensity (apo-BF1): 1.51). It might be due to changes in the microenvironment of Trp90 and Trp126, caused by a weak calcium binding in the kringle domain.[3,6,7] Though the X-ray structure did not locate such a binding site, Hamaguchi and co-workers suggested the existence of two sites promising calcium binding. One of these sites, involving Ser121, Thr123, and Gly124, may influence the orientation of Trp126 and, therefore, influence the tryptophan-quencher interactions. However, since the X-ray structure does not show a weak calcium binding site and the DAS of components A and C are identical for apo- and Ca-BF1, an influence of calcium binding on the Trp126 orientation appears to be very speculative.

The important feature of the observed disulfide-tryptophan interaction in BF1 for the understanding of the prothrombinase is an involvement of this interaction in membrane binding. The Gla residues Gla20 and Gla21, which are supposed to be responsible for the calcium-bridged membrane binding, are part of the Cys18–Cys23 hexapeptide disulfide loop. On the other hand, the calcium-induced conformational change, which is essential for membrane binding, leads to an equilibrium interaction of this disulfide linkage with Trp42. The necessity of the Cys18–Cys23 disulfide, as well as of the aromatic cluster formed by Phe41, Trp42, and Tyr45 for membrane binding ability of BF1 and of homologous proteins was also demonstrated by investigations of modified proteins.[20,57,58] We propose, that the characterization of the Trp42 fluorescence together with the determination of the monomolecular equilibrium constant can be a new method for monitoring conformational changes in the Gla domain of BF1 and of related proteins, induced by membrane binding. In progressing experiments, this method is used to find a molecular mechanistic explanation for the unique position of phosphatidyl-L-serine among the procoagulant lipids in the process of calcium-chelat formation by a polar phospholipid headgroup and Gla residues of the protein.[59,60]

## CONCLUSIONS

The presented time-resolved tryptophan fluorescence study provides a tool to investigate separately structural changes in Gla and kringle domain of BF1 without cleaving the protein into smaller fragments or modifying the protein by site-directed mutagenesis. Calcium addition does not change the microenvironment of the kringle tryptophans, but establishes an equilibrium between a non-fluorescent adduct formed by the Gla tryptophan and a disulfide bridge and the "free" species. Experimental work[20,57,58] and structural data[3,5] indicate a direct involvement of this equilibrium in the binding to phospholipid membranes. Together with the fact that BF1 is an good model for studying the membrane binding behavior of prothrombin,[61] these conclusions motivate the use of this method in the investigation of the special role of the prothrombin-calcium-phosphatidyl-L-serine interaction in the prothrombinase.[59,60]

## ACKNOWLEDGMENTS

We thank Pola Berkowitz and Dr. Kenny Pearce for the preparation of BF1; Drs. Nancy Thompson, Richard Hiskey, Jim Longworth, Kenny Pearce, Stefan Vajda, and Jiri Hudecek for discussions; Mark Schmidt and Petr Kapusta for experimental assistance; Dr. Dirk Näther for the measurements of the fluorescence decays of the four standards; and Edinburgh Analytical Instruments for providing analysis programs. M.H. is a recipient of the "Liebig"-stipend of the "Fonds der Chemischen Industrie," V.F. is a recipient of the "Fullbright Award Scholarship" and acknowledges partial financial support from grant 301/93/1100 GACR.

## REFERENCES

1. Suttie, J.W., Jackson, C.M. Prothrombin structure, activation and biosynthesis. Physiol. Rev. 57:1–70, 1977.
2. Soriano-Garcia, M., Park, C.H., Tulinsky, A., Ravichandran, K.G., Skrzypczak-Jankun, E. Structure of $Ca^{2+}$ pro-

thrombin fragment 1 including the conformation of the Gla domain. Biochemistry 28:6805–6810, 1989.
3. Hamaguchi, N., Charifson, P., Darden, T., Xiao, L., Padmanabhan, K., Tulinsky, A., Hiskey, R.G., Pedersen, L.G. Molecular dynamics simulations of bovine prothrombin fragment 1 in the presence of calcium ions. Biochemistry 31:8840–8848, 1992.
4. Seshardi, T.P., Tulinsky, A., Skrzypczak-Jankun, R., Park, C.H. Structure of bovine prothrombin fragment 1 refined at 2.25 A resolution. J. Mol. Biol. 220:481–494, 1991.
5. Soriano-Garcia, M., Padmanabhan, K., de Vos, A.M., Tulinsky, A. The $Ca^{2+}$ ion and membrane binding structure of the Gla domain of Ca-prothrombin fragment 1. Biochemistry 31:2554–2566, 1992.
6. Lundblad, R. A hydrophobic site in human prothrombin present in a calcium-stabilized conformer. Biochem. Biophys. Res. Commun. 157:295–300, 1988.
7. Berkowitz, P., Huh, N.-W., Brostrom, K.E., Panek, M.G., Weber, D.J., Tulinsky, A., Pedersen, L.G., Hiskey, R.G. A metal ion-binding site in the kringle region of bovine prothrombin fragment 1. J. Biol. Chem. 267:4570–4576, 1992.
8. Bloom, J.W., Mann, K.G. Metal ion induced conformational transitions of prothrombin and prothrombin fragment 1. Biochemistry 17:4430–4438, 1978.
9. Nelsestuen, G.L. Role of γ-carboxyglutamic acid. An unusual transition required for calcium-dependent binding to phospholipids. J. Mol. Biol. 251:5648–5656, 1976.
10. Prendergast, F.G., Mann, K.G. Differentiation of metal-ion induced transitions of prothrombin fragment 1. J. Biol. Chem. 252:840–850, 1977.
11. Marsh, H.C., Scott, M.E., Hiskey, R.G., Koehler, K.A. The nature of the slow metal ion-dependent conformational transitions in bovine prothrombin. Biochem. J. 183:513–517, 1979.
12. Astermark, J., Björk, I, Öhlin, A., Stenflo, J. Structural requirements for $Ca^{2+}$ binding to the γ-carboxyglutamic acid and epidermal growth factor-like regions of factor IX. J. Biol. Chem. 266:2430–2437, 1991.
13. Astermark, J., Hogg, P.J., Björk, I., Stenflo, J. Effects of γ-carboxyglutamic acid and epidermal growth factor-like modules of factor IX of factor X activation. J. Biol. Chem. 267:3249–3256, 1991.
14. Persson, E.J., Björk, I., Stenflo, J. Protein structural requirements for $Ca^{2+}$ binding to light chain of factor X. J. Biol. Chem. 266:2444–2452, 1991.
15. Eftink, M.R.. Fluorescence techniques for studying protein structure. In: "Protein Structure Determination: Methods of Biochemical Analysis," vol. 35. Suelter C.H., (ed.). New York: John Wiley & Sons, Inc., 1991:127–205.
16. Demchenko, A.P. Fluorescence and dynamics in proteins. In: "Topics in Fluorescence Spectroscopy: Biochemical Applications," vol. 3. Lakowicz, J.R. (ed.). New York: Plenum Press, 1992:65–106.
17. Demas, J.N. "Excited State Lifetime Measurements." New York: Academic Press, 1983.
18. O'Connor, D.V., Phillips, D. "Time-Correlated Single Photon Counting." London: Academic Press, 1984.
19. Mann, K.G. Blood clotting enzymes: prothrombin. Methods Enzymol. 45:123–156, 1977.
20. Pollock, J.S., Shepard, A.J., Weber, D.J., Olson, D.L., Klapper, D.G., Pedersen, L.G., Hiskey, D.G. Phospholipid binding properties of bovine prothrombin peptide residues 1–45. J. Biol. Chem. 263:14216–14223, 1988.
21. Tendian, S.W., Lentz, B.R. Evaluation of membrane phase behaviour as a tool to detect extrinsic protein-induced domain formation: Binding of prothrombin to PS/PC vesicles. Biochemistry 29:6720–6729, 1990.
22. Chang, M.C., Coutney, S.H., Cross, A.J., Gulotty, R.J., Petrich, J.W., Fleming, G.R. Time correlated single photon counting with microchannel plate detectors. Anal. Instrum. 14:433–464, 1985.
23. Hansen, J.E., Longworth, J.W., Fleming, G.R. Photophysics of metalloazurins. Biochemistry 29:7329–7338, 1990.
24. Marquardt, D.W. An algorithm for least-squares estimation of nonlinear parameters. J. Soc. Ind. Appl. Math. 11: 431–441, 1963.
25. Hof, M., Schleicher, J., Schneider, F.W. Time-resolved fluorescence in doped aerogels and organosilicate glasses. Ber. Bunsenges. Phys. Chem. 93:1377–1381, 1989.
26. Siano, D.B., Metzler, D.E. Band shapes of the electronic spectra of complex molecules. J. Chem. Phys. 51:1856–1861, 1969.
27. James, D.R., Demmer, D.R., Steer, R., Verral, E. Fluorescence lifetime quenching and anisotropy studies of ribonuclease T1. Biochemistry 24:5517–5526, 1985.
28. Chen, L.X., Longworth, J.W., Fleming, G.R. Picosecond time-resolved fluorescence of ribonuclease T1. Biophys. J. 51:865–873, 1987.
29. Alcala, J.R., Gratton, E., Prendergast, F.G. Interpretation of fluorescence decays in proteins using continuous lifetime distributions. Biophys. J. 51:925–936, 1987.
30. Rosato, N., Gratton, E., Mei, G., Finazzi-Agro, A. Fluorescence lifetime distribution in human superoxide dismutase. Biophys. J. 58:817–822, 1990.
31. Zolese, G., Giambanco, I., Curatola, G., Donato, R. Time-resolved fluorescence of S-100a protein in the absence and presence of calcium and phospholipids. Biochim. Biophys. Acta 1162:47–53, 1993.
32. Kim, S., Chowdhury, F.N., Stryjewski, W., Younathan, E.S., Russo, P.S., Barkley, M.D. Time-resolved fluorescence of the single tryptophan of *bacillus staerothermophilus* phosphofructokinase. Biophys. J. 65:215–226, 1993.
33. Petrich, J.W., Longworth, J.W., Fleming, G.R. Internal motion and electron transfer in proteins: A picosecond fluorescence study of three homologous azurins. Biochemistry 26:2711–2722, 1987.
34. Eftink, M.R., Wasylewski, Z., Ghiron, C.A. Phase-resolved spectral measurements with several two tryptophan containing proteins. Biochemistry 26:8338–8346, 1987.
35. Eisinger, J., Feuer, B., Lamola, A.A. Intramolecular singlet excitation transfer. Applications to polypeptides. Biochemistry 8:3908–3915, 1969.
36. DeToma, R.P., Easter, J.H., Brand, L. Dynamic interactions of fluorescence probes with the solvent environment. J. Am. Chem. Soc. 98:5001–5007, 1976.
37. Grinvald, A., Steinberg, I.Z. Fast relaxation processes in a protein revealed by the decay kinetics of tryptophan fluorescence. Biochemistry 13:5170–5177, 1974.
38. Harris, D.L., Hudson, B.S. Photophysics of tryptophan in bacteriophage T4 lysozymes. Biochemistry 29:5276–5285, 1990.
39. Eftink, M.R., Wasylewski, Z. Fluorescence lifetime and solute quenching with the single tryptophan containing protein parvalbumin from codfish. Biochemistry 28:382–391, 1989.
40. Royer, C.A. Investigation of the structural determinants of the intrinsic fluorescence emission of the *trp* repressor using single tryptophan mutants. Biophys. J. 63:741–750, 1992.
41. Szabo, A.G., Stepanik, T.M., Wayner, D.M., Young, N.M. Conformational heterogeneity of the copper binding site in azurin. A time-resolved study. Biophys. J. 41:244–249, 1983.
42. Ludescher, R.D., Wolwerk, J.J., de Haas, K.H., Hudson, B.S. Complex photophysics of the single tryptophan of porcine pancreatic phospholipase $A_2$, its zymogen, and an enzyme/micelle complex. Biochemistry 24:7240–7249, 1985.
43. Werner, T.C., Foster, L.S. The fluorescence of tryptophanyl peptides. Photochem. Photobiol. 29:905–914, 1979.
44. Yu, H.T., Colucci, W.J., McLaughlin, P., Barkley, M.D. Fluorescence quenching in indoles by excited-state proton transfer. J. Am. Chem. Soc. 114:8449–8454, 1992.
45. Castelli, F., White, H.D., Foster, L.S. Lifetime and quenching of tryptophan fluorescence in whiting parvalbumin. Biochemistry 27:3366–3372, 1988.
46. Vincent, M., Brochon, J.C., Merola, M., Jordi, W., Gallay, J. Nanosecond dynamics of horse heart apocytochrome *c* in aqueous solution as studied by time-resolved fluorescence of the single tryptophan residue (Trp-59). Biochemistry 27: 8752–8761, 1988.
47. Hutnik, C.M., Szabo, A.G. Confirmation that multiexponential fluorescence decay behaviour of holoazurin originates from conformational heterogeneity. Biochemistry 28:3923–3934, 1989.
48. Atkins, W.M., Stayton, P.S., Villafranca, J.J. Time-resolved fluorescence studies of genetically engineered *Escherichia coli* glutamine synthetase. Effects of ATP on the tryptophan 57 loop. Biochemistry 30:3406–3416, 1991.
49. Chabbert, M., Lukas, T.L., Watterson, D.M., Axelsen, P.H.,

Prendergast, F.G. Fluorescence analysis of calmodulin mutants containing tryptophan: Conformational changes induced by calmodulin-binding peptides from myosin light chain kinase and protein kinase II. Biochemistry 30:7615–7630, 1991.
50. Elofsson, A., Rigler, R., Nilsson, L., Roslund, J., Krause, G., Holmgren, A. Motions of aromatic side chains, picosecond fluorescence, and internal energy transfer in *Escherichia coli* thioredoxin studies by site-directed mutagenesis, time-resolved fluorescence spectroscopy and molecular dynamic simulations. Biochemistry 30:9648–9655, 1991.
51. Liao, R., Wang, C.R., Cheung, H.C. Time-resolved tryptophan emission study of cardiac troponin I. Biophys. J. 63:986–995, 1992.
52. Li, Z., Bruce, A., Galley, W.C. Temperature dependence of the disulfide perturbation of the triplet sate of tryptophan. Biophys. J. 61:1364–1371, 1992.
53. Schlyer, B.D., Lau, E., Maki, A.H. A comparative investigation of snake venon neurotoxins and their triplet-state tryptophan-disulfide interactions using phosphorescence and optically detected magnetic resonance. Biochemistry 31:4375–4383, 1992.
54. Vande Ven, M., Han, M., Walbridge, D., Knutson, J., Shin, D., Afinsen, R., Brand, L. Fluorescence decay studies of thioredoxin: Quenching, oxidation and reduction [abstr]. Biophys. J. 51:275a, 1987.
55. Swadesh, J.K., Mui, P.W., Scheraga, H.A. Thermodynamics of the quenching of tyrosyl fluorescence by dithiothreitol. Biochemistry 26:5761–5769, 1987.
56. Sanyal, G., Kim, E., Thompson, F.M., Brady, K.E. Static quenching of tryptophan fluorescence by oxidized dithiothreitol. Biochem. Biophys. Res. Commun. 165:772–781, 1989.
57. Schwalbe, R.A., Ryan, J., Stern, D.M., Kisiel, W., Dahlback, D., Nelsestuen, G.L. Protein structural requirements and properties of membrane binding by γ-carboxyglutamic acid-containing. J. Biol. Chem. 264:20288–20296, 1989.
58. Zhang, L., Castellino, F.J. Role of the hexapeptide disulfide loop present in the γ-carboxyglutamic acid domain of human protein C in its activation properties and in the in vitro anticoagulant activity of activated protein C. Biochemistry 30:6696–6704, 1991.
59. Gerads, I., Govers-Riemslag, J.W.P., Tans, G., Zwaal, R.F.A., Rosing, J. Prothrombin activation on membranes with anionic lipids containing phosphate, sulfate, and/or carboxyl groups. Biochemistry 29:7967–7974, 1990.
60. Comfurius, P., Smeets, E.F., Willems, G.M., Bevers, E.M., Zwaal, R.F.A. Assembly of the prothombinase complex on lipids vesicles depends on the streochemical configuration of the polar headgroup of phosphatidylserine. Biochemistry 33:10319–10324, 1994.
61. Pearce, K.H., Hof, M., Lentz, B.R., Thompson N.L. Comparison of the membrane binding kinetics of bovine prothrombin and its fragment 1. J. Biol. Chem. 268:22984–22991, 1993.